J. Fluid Mech. (2019), *vol.* 874, *pp.* 131–157.
doi:10.1017/jfm.2019.415

Weak shock reflection in channel flows for dense gases

A. Kluwick[1],† **and E. A. Cox**[2]

[1]Institute of Fluid Dynamics and Heat Transfer, Vienna University of Technology, Tower BA/E322, Getreidemarkt 9, 1060 Vienna, Austria

[2]School of Mathematics and Statistics, Science Centre North, University College Dublin, Belfield, Dublin 4, Ireland

(Received 21 September 2018; revised 7 May 2019; accepted 16 May 2019; first published online 3 July 2019)

The canonical problem of transonic dense gas flows past two-dimensional compression/expansion ramps has recently been investigated by Kluwick & Cox (*J. Fluid Mech.*, vol. 848, 2018, pp. 756–787). Their results are for unconfined flows and have to be supplemented with solutions of another canonical problem dealing with the reflection of disturbances from an opposing wall to finally provide a realistic picture of flows in confined geometries of practical importance. Shock reflection in dense gases for transonic flows is the problem addressed in this paper. Analytical results are presented in terms of similarity parameters associated with the fundamental derivative of gas dynamics (Γ), its derivative with respect to the density at constant entropy (Λ) and the Mach number (M) of the upstream flow. The richer complexity of flows scenarios possible beyond classical shock reflection is demonstrated. For example: incident shocks close to normal incidence on a reflecting boundary can lead to a compound shock–wave fan reflected flow or a pure wave fan flow as well as classical flow where a compressive reflected shock attached to the reflecting boundary is observed. With incident shock angles sufficiently away from normal incidence regular reflection becomes impossible and so-called irregular reflection occurs involving a detached reflection point where an incident shock, reflected shock and a Mach stem shock which remains connected to the boundary all intersect. This triple point intersection which also includes a wave fan is known as Guderley reflection. This classical result is demonstrated to carry over to the case of dense gases. It is then finally shown that the Mach stem formed may disintegrate into a compound shock–wave fan structure generating an additional secondary upstream shock. The aim of the present study is to provide insight into flows realised, for example, in wind tunnel experiments where evidence for non-classical gas dynamic effects such as rarefaction shocks is looked for. These have been predicted theoretically by the seminal work of Thompson (*Phys. Fluids*, vol. 14 (9), 1971, pp. 1843–1849) but have withstood experimental detection in shock tubes so far, due to, among others, difficulties to establish purely one-dimensional flows.

Key words: gas dynamics, shock waves, high-speed flow

† Email address for correspondence: alfred.kluwick@tuwien.ac.at

1. Introduction

The possibility that solutions of the governing equations for compressible inviscid flows may exhibit jump discontinuities was proposed by Stokes (1848). Following severe criticism by, among others, Rayleigh, in 1877 the proposal was retracted by Stokes. Arguments in support of shock discontinuities were however provided by Earnshaw (1860) and by Rankine (1870) and Hugoniot (1887, 1889) and form the basis of the present theory of jump discontinuities or shocks. Readers interested in the history of these early developments are referred to the historical reviews of Johnson & Chéret (1998) and Kluwick (2018). The main point to be made in this connection has been formulated most clearly in the paper 'A History of Shock Waves' by Krehl (2001). In summary:

> 'The puzzling shock wave, characterised by a stepped wave front, was difficult to accept by early naturalists because it involved the abandonment of the principle 'Natura non facit saltus'. Surprisingly, however, the problem was tackled neither by experimentalists nor philosophers but rather by mathematical physicists. Jouget wrote: "the shock wave represents a phenomenon of rare peculiarity such that it has been uncovered by the pen of mathematicians, first by Riemann, then by Hugoniot. The experiments followed afterwards"'.

This statement which then applied exclusively to the class of perfect gases now is also known to hold for gases having arbitrary equations of state. This is due to more recent developments starting with the pioneering work by Bethe (1942). Most importantly he (obviously being unaware of earlier work by Becker (1922)) recognised that shocks may be of expansive rather than compressive type in fluids which exhibit regions of negative isentropic curvature in the pressure, specific volume diagram. In addition he also recognised that this is possible for fluids having large values of specific heat at constant volume (c_v) relative to the universal gas constant (R), i.e. having complex molecules with a large number of internal degrees of freedom. An estimate based on the van der Waals equation of state indicated that such shocks may form in fluids if $c_v/R > 17.5$ (a result obtained slightly later also by Zeldovich (1946)). A result which Bethe considered unrealistic. This point of view was contested later by Thompson and coworkers who identified a number of candidates for dense gases which might exhibit negative isentropic curvature in the general neighbourhood of the thermodynamic critical point (see Thompson (1971) and Thompson & Lambrakis (1973)). Measures of isentropic curvature had already been proposed earlier (Duhem 1909) but its non-dimensional version proposed by Thompson (1971) namely

$$\Gamma(\rho, s) = \frac{1}{c}\left.\frac{\partial(c\rho)}{\partial\rho}\right|_s, \tag{1.1}$$

where ρ, s and c are respectively fluid density, entropy and sound speed, is now commonly used. As Γ plays a predictive role in most areas of compressible flows it is frequently referred to as the fundamental derivative of gas dynamics. When Γ is small its variation with density ρ becomes important in determining the nature of the flow and this is given by the parameter

$$\Lambda(\rho, s) = \rho\left.\frac{\partial\Gamma}{\partial\rho}\right|_s. \tag{1.2}$$

Because of the pioneering research of Bethe, Zel'dovich and Thompson it is now common to identify fluids that exhibit negative Γ regions as BZT-fluids.

In passing we mention that theoretical work also suggests a second mechanism which generates states having $\Gamma < 0$ in the two phase region close to the thermodynamic critical point. This second mechanism is associated with the divergence of the isochoric heat capacity as the thermodynamical critical point is approached, see e.g. Kluwick (2001) and the more recent study Nannan, Guardone & Colonna (2013). In what follows we exclude critical point phenomena and concentrate on effects caused by high molecular complexity in the single phase region.

The analysis and results presented in this paper are for fluid flows in the pressure, specific volume (V) plane close to the $\Gamma = 0$ curve. For particular BZT fluids such as PP10 ($C_{13}F_{22}$) this curve has been computed based on sophisticated model equations of state. The highlighted gas PP10 has a complex fluorinated molecular structure and has been used as a working fluid in BZT shock tube experiments, (Fergason, Guardone & Argrow 2003). Qualitative estimates of pressure, specific volume and temperature associated with a negative Γ region have also been obtained for different BZT fluids using various thermodynamic models that includes the Martin–Hou, Soave–Redlich–Kwong and Peng–Robinson model equations of state, see Guardone, Vigevano & Argrow (2004). Strong agreements between computational models are observed and the negative Γ region of a BZT fluid is estimated to be within the ranges $0.75 < P/P_c < 1.0$, $1.4 < V/V_c < 2.5$ and $0.96 < T/T_c < 1.01$ where the subscript c denotes critical point values. BZT fluid flows in experiments that extend into these ranges, crossing the $\Gamma = 0$ curve, are expected to exhibit phenomena similar to those described in this paper.

We should note that by assuming $\Lambda = O(1)$ we exclude a small region of the P, V plane lying close to where the $\Gamma = 0$ curve is tangent to the isentrope. Modelling the flow in this region requires addition terms in the derived model equations similar to those obtained in Kluwick (1993) for transonic nozzle flow.

Extensive theoretical studies elaborating on the non-classical and often counter-intuitive behaviour of BZT fluids, including the possible formation of rarefaction shocks, followed the stimulating work of Thompson (1971). Early investigations concentrated on unsteady flow phenomena which are not at the core of the present study. Readers interested in this field of research are referred to recent reviews, (Kluwick 2017, 2018). The present study focuses on a well-defined specific problem of steady inviscid dense gas flow and, therefore, is not intended to provide a complete account of the rapidly growing literature in general. To put our work in perspective, however, we briefly address important other areas such as unconfined flows, flows past single airfoils as well as nozzle and cascade configurations which have been studied among others by Cramer & Tarkenton (1992), Cramer & Fry (1993), Kluwick (1993), Monaco, Cramer & Watson (1997), Wang & Rusak (1999), Rusak & Wang (2000), Cinella & Congedo (2005), Congedo, Corre & Cinella (2007), Guardone, Zamfirescu & Colonna (2010), Gori, Vimercati & Guardone (2017), Vimercati, Kluwick & Guardone (2018).

Unfortunately, efforts to support the theoretical predictions that rarefaction shocks may form in negative Γ fluids by experimental evidence have failed so far. But although fully developed single phase planar rarefaction shocks have not yet been observed in shock tubes, some recent work carried out at the FAST (Flexible Asymmetric Shock Tube) facility of the DTU in Delft points to the existence of 'embryo' negative Γ shocks, (Mathijssen 2017). This work, however, also reveals significant challenges for the search of the 'holy grail' of rarefaction shocks using

shock tubes. Thermodynamic states which can be realised at present have $|\Gamma| \ll 1$, i.e. isentropes just barely enter the negative Γ region. Rarefaction shocks expected to form thus will be weak and extremely sensitive to disturbances resulting from deviations from one-dimensional flow conditions caused primarily by fast opening devices such as punched diaphragms or valves. In contrast, experimental investigations of shocks under steady flow conditions will not be contaminated by such disturbances and therefore represent a promising alternative – hence the motivation for the present paper where the canonical problem of shock reflection is of primary interest. The associated wave reflection pattern then results from two building blocks – oblique shock fronts and centred wave fans which simplifies both the theoretical analysis and the interpretation of experimental data.

A complete picture of phenomena to be expected in the limit of small disturbances with special emphasis on the transonic flow regime where dense gas effects are most pronounced has recently been given by Kluwick & Cox (2018), while fully nonlinear solutions have been obtained numerically by Vimercati *et al.* (2018). Their results are for an oblique shock in an unconfined flow and have to be supplemented with solutions of another canonical problem dealing with the reflection of disturbances from an opposing solid wall to finally provide a realistic picture of phenomena arising in confined geometries of practical importance.

The present study of the reflection problem is based on the assumptions formulated in Kluwick & Cox (2018) which are briefly summarised in § 2. Extensions required to treat shock reflections are also derived in § 2, where it is shown that solutions depend on a set of three non-dimensional parameters which characterise, respectively, the strength of the incoming shock, the Mach number range where transonic effects are of importance and the influence of dense gas behaviour. Based on these parameters different regimes of regular and irregular reflections are identified and analysed in §§ 3 and 4. Finally § 5 summarises the main achievements of the present work and addresses open questions which require further efforts.

2. Formulation

We consider the problem of steady shock wave reflection in a channel as sketched in figure 1. Uniform supersonic flow is incident on a thin wedge located in a channel wall and the shock wave generated is reflected off the opposite facing wall. The channel is of width H, the wedge has an inclination angle $\theta \approx a\delta \ll 1$ and the upstream supersonic uniform flow $\boldsymbol{u} = (u_\infty, 0)$ is aligned with the x axis and the channel axis. The wedge geometry introduces a small asymptotic parameter $\delta > 0$ for the problem with the order-one parameter a providing, in the asymptotic model, a measure of the inclination of the wedge. The flow generated by the wedge is described in terms of the velocity $\boldsymbol{u} = (u, v)$ non-dimensionalised with the free-stream velocity and involves a perturbed velocity with components $(\tilde{u}, \tilde{v})$ given by

$$\frac{u}{u_\infty} = 1 + \frac{\delta^{2/3}}{\Gamma_\infty^{1/3}}\tilde{u} + o(\delta^{1/2}), \tag{2.1}$$

$$\frac{v}{u_\infty} = \delta\ \mathrm{sgn}(\Gamma_\infty)\tilde{v} + o(\delta), \tag{2.2}$$

where we have assumed that Γ given by (1.1) evaluated in the free-stream reference state and denoted by Γ_∞ is $O(\delta^{1/2})$. This perturbed flow $(\tilde{u}, \tilde{v})$ can be shown to satisfy the transonic small disturbance equations formulated here for BZT fluids as

$$\frac{\partial j}{\partial \xi} + \frac{\partial \tilde{v}}{\partial \eta} = 0, \quad j = -K_1\tilde{u} - \tilde{u}^2 + \frac{K_2}{3}\tilde{u}^3, \tag{2.3a,b}$$

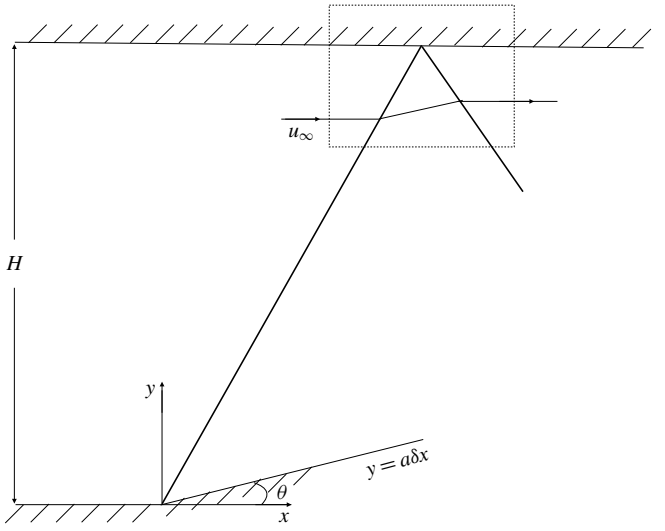

FIGURE 1. Flow geometry for reflection of a plane shock generated by a wedge located at $x = 0, y = 0$ with inclination $a\delta > 0$ in a channel of width H.

$$\frac{\partial \tilde{u}}{\partial \eta} - \frac{\partial \tilde{v}}{\partial \xi} = 0, \tag{2.4}$$

with the scaled non-dimensional channel coordinates

$$\xi = \delta^{-1/3} |\Gamma_\infty|^{-1/3} \frac{x}{H}, \quad \eta = \frac{y}{H}, \quad \delta \ll 1, \tag{2.5a,b}$$

which account for rapid variations in the x coordinate compared to y, consistent with the near normal orientation of incident and reflected shocks.

The order-one similarity parameters K_1 and K_2 are given by

$$K_1 = \frac{M_\infty^2 - 1}{(\delta \Gamma_\infty)^{2/3}}, \quad K_2 = \frac{\delta^{2/3} \Lambda_\infty}{\Gamma_\infty^{4/3}}, \tag{2.6a,b}$$

where K_1 is a rescaled transonic similarity parameter with $M_\infty = u_\infty / c_\infty$ the Mach number of the unperturbed upstream flow defined using c_∞ the upstream unperturbed sound speed. The parameter K_2 with $\Lambda_\infty = \Lambda(\rho_\infty, s_\infty) = O(1)$ measures the relevant importance of cubic and quadratic nonlinearity, see Cramer & Tarkenton (1992) for details. The choice of scalings leading to (2.3)–(2.6) ensure that the formulation reduces to the classical case when $\Gamma_\infty = O(1)$ see Cole & Cook (1986). Equations (2.3)–(2.6) were first derived in Cramer & Tarkenton (1992) in the context of steady transonic flow over thin airfoils and more recently in Kluwick & Cox (2018) for flow over a wedge.

To the authors' knowledge evolution equations exhibiting both quadratic and cubic nonlinearity were first studied for the simpler case of unsteady planar waves, e.g. Cramer & Kluwick (1984). Extensions to more complex geometries are discussed in Kluwick (1991) which also includes an example of purely cubic nonlinearity, see also Lee-Bapty & Crighton (1987).

Just as in the classical case the modified transonic small disturbance equations (2.3), (2.4) arises as a distinguished asymptotic limit for the Euler equations leading to the estimates

$$\frac{u-u_\infty}{u_\infty}=O(\delta^{1/2}),\quad \frac{v}{u_\infty}=O(\delta),\quad M_\infty^2-1=O(\delta), \tag{2.7a–c}$$

and differing from the classical results due to the assumption that $\Gamma_\infty=O(\delta^{1/2})$ and $\Lambda_\infty=O(1)$ which ensures that both K_1 and K_2 are $O(1)$. Consistent with the asymptotic scalings in (2.7) we construct solutions of (2.3), (2.4) satisfying the asymptotic boundary conditions

$$\text{on } \eta=0: \quad \tilde{v}=0,\ \xi<0, \tag{2.8a}$$

$$\tilde{v}=a\ \mathrm{sgn}(\Gamma_\infty),\ \xi>0, \tag{2.8b}$$

$$\text{on } \eta=1: \quad \tilde{v}=0,\ -\infty<\xi<\infty. \tag{2.8c}$$

In other words solutions to the transonic small disturbance equations (2.3), (2.4) are sought so that the incident shock generated by the wedge deflects the flow to $\tilde{v}=a\ \mathrm{sgn}(\Gamma_\infty)$. After reflection from the boundary at $\eta=1$ the flow must then satisfy the downstream condition $\tilde{v}=0$.

The basic building blocks used to construct the flows generated include shock waves and centred simple waves. If we first consider shock waves: denoting the jump in a flow property β across a shock as $[\beta]=\beta_2-\beta_1$, where subscripts 1 and 2 reference upstream and downstream states, then it is readily established that across a shock we have

$$\frac{[\tilde{v}]}{[\tilde{u}]}=\pm\sqrt{-\frac{[j]}{[\tilde{u}]}},\quad j=-K_1\tilde{u}-\tilde{u}^2+\frac{K_2}{3}\tilde{u}^3. \tag{2.9a,b}$$

Details can be found in Kluwick & Cox (2018). It is useful to introduce a scaled Mach number for the flows associated with a shock jump. As shown in Kluwick & Cox (2018) the local Mach number M satisfies

$$2\frac{(M-1)}{(\delta\Gamma_\infty)^{2/3}}=K_1+2\tilde{u}-K_2\tilde{u}^2=-\frac{\mathrm{d}j}{\mathrm{d}\tilde{u}}. \tag{2.10}$$

With supersonic flow upstream, shock jumps described by (2.9) may involve supersonic–supersonic or supersonic–subsonic jump transitions as calculated from (2.10).

The so-called shock polar curve is a plot derived from (2.9) of all possible downstream states $(\tilde{u}_2,\ \tilde{v}_2)$ that can be connected to a given fixed upstream state $(\tilde{u}_1,\ \tilde{v}_1)$ by a shock jump. This is illustrated in figure 2(*a*) for the case $K_1=1$, $K_2=-0.8$ and upstream state $\tilde{u}_1=0$, $\tilde{v}_1=0$ i.e. we plot

$$\tilde{v}_2(\tilde{u}_2)=-\tilde{u}_2\sqrt{K_1+\tilde{u}_2-\frac{K_2}{3}\tilde{u}_2^2}. \tag{2.11}$$

With decreasing values of the downstream velocity $\tilde{u}_2$, i.e. increasing shock strength, we see a shock transition S_1 from a supersonic–supersonic shock to a supersonic–subsonic shock S_2.

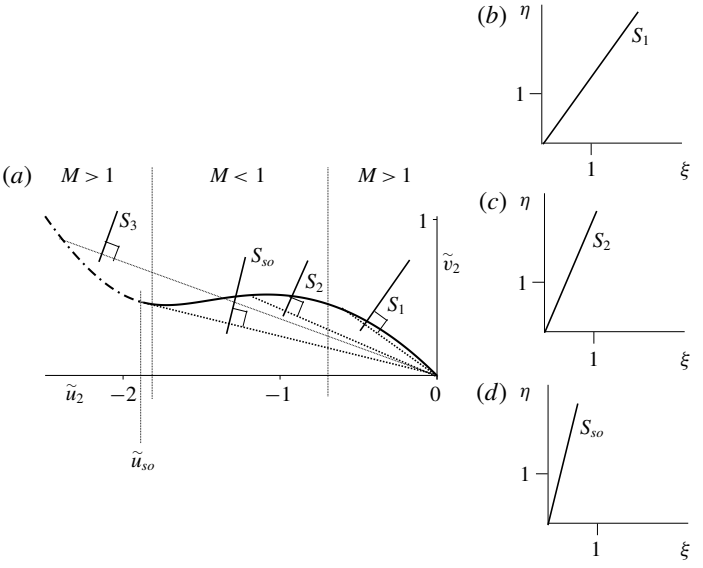

FIGURE 2. (*a*) Shock polar for $K_1 = 1$, $K_2 = -0.8$ with the construction of shocks S_1, S_2, S_{so}, S_3 of increasing strength. The shock S_{so} corresponds to downstream sonic conditions $\tilde{u}_2 = \tilde{u}_{so}$ and the possible shock S_3 violates the speed ordering condition. In (*b–d*) the corresponding shocks in the ξ, η plane are plotted with the shocks shown in (*a*) to be orthogonal to the shock chord (Rayleigh line) in the polar plot.

If the shock surface is located at $\eta = \eta_s(\xi)$ then integrating (2.3), (2.4) across the shock discontinuity leads to a shock slope given by

$$\frac{\mathrm{d}\eta_s}{\mathrm{d}\xi} = \mp \frac{1}{\sqrt{-\dfrac{[j]}{[\tilde{u}]}}}, \tag{2.12}$$

where we observe the useful geometric construction that the slope of the chord in the $(\tilde{u}, \tilde{v})$ hodograph plane, connecting upstream states $(\tilde{u}_1, \tilde{v}_1)$ to downstream states $(\tilde{u}_2, \tilde{v}_2)$, given by $[\tilde{v}]/[\tilde{u}]$ in (2.9) is orthogonal to the shock slope $\mathrm{d}\eta_s/\mathrm{d}\xi$ in the (η, ξ) plane with appropriately chosen signs. This construction is illustrated in figure 2(*a*) and the orientation of the shocks S_1, S_2 in the physical (ξ, η) plane is shown in figures 2(*b*) and 2(*c*).

Not all jump discontinuities described by (2.9) lead to physically acceptable shock solutions. We require in addition the imposing of criteria to eliminate non-physical solutions. A fundamental requirement is that that entropy does not decrease across a shock i.e. $[s] \geqslant 0$ which leads to the constraint $\tilde{u}_2 \leqslant \tilde{u}_1$, see Kluwick & Cox (2018). Only portions of the solution curve of (2.9) satisfying the entropy jump condition are plotted in figure 2(*a*). It was shown by Cramer & Kluwick (1984) in the context of BZT fluids with $|\Gamma| \ll 1$ and $\Lambda = O(1)$ that the entropy condition is too weak to rule out certain inadmissible supersonic–supersonic shock discontinuities, where inadmissibility is understood in terms of shocks for which no thermoviscous profile can be constructed. It was shown that in addition a wave speed ordering condition must be imposed.

We develop this condition, applicable to supersonic–supersonic shock jumps, by first noting that characteristics of (2.3), (2.4) have slopes in the (ξ, η) plane given by

$$\frac{\mathrm{d}\eta}{\mathrm{d}\xi} = \mp \frac{1}{\sqrt{-\dfrac{\mathrm{d}j}{\mathrm{d}\tilde{u}}}}, \tag{2.13}$$

and we then require that the shock slope lies between the characteristic slopes of flow states generating the shock i.e.

$$\sqrt{-\left.\frac{\mathrm{d}j}{\mathrm{d}\tilde{u}}\right|_1} \geqslant \sqrt{-\frac{[j]}{[\tilde{u}]}} \geqslant \sqrt{-\left.\frac{\mathrm{d}j}{\mathrm{d}\tilde{u}}\right|_2}. \tag{2.14}$$

Results are stated here for forward orientated waves (i.e. $\mathrm{d}\eta/\mathrm{d}\xi > 0$) and holding for $-\mathrm{d}j/\mathrm{d}\tilde{u}|_{1,2} > 0$ which ensures that the characteristics are real and the flow is supersonic ahead and behind the shock. Shocks where one of the equalities in (2.14) holds are termed 'sonic shocks', see Kluwick (2001). Equation (2.14) is recognised as the Lax entropy condition and when one of the equalities is satisfied the shocks are also referred to as a left or right contact shocks, see Dafermos (2005). The possibility of 'sonic shocks' (contact shocks) occurring has no classical gas dynamics counterpart – the shock condition given in (2.14) reduces on setting $K_2 = 0$ to

$$\sqrt{K_1 + 2\tilde{u}_1} > \sqrt{K_1 + \tilde{u}_1 + \tilde{u}_2} > \sqrt{K_1 + 2\tilde{u}_2}, \tag{2.15}$$

which is the well-known classical ideal gas case, with strict inequalities applying, see Cole & Cook (1986). Also and in contrast to the non-classical gas case this wave speed ordering condition when applied is simply equivalent to the selection rule $[s] \geqslant 0$ rather than a further constraint.

In figure 2(*a*) the shock labelled S_3 represents jumps to downstream states $\tilde{u}_2$, $\tilde{v}_2$ (plotted as a dashed curve) constructed from (2.11) which satisfies $[s] > 0$ or equivalently $M_2 < M_1$ but violates the speed ordering condition (2.14). There is a limiting shock strength $\tilde{u}_{so}$ where 'sonic' conditions hold downstream and represented by shock S_{so} in figures 2(*a*) and 2(*d*). The supersonic state $\tilde{u}_{so}$ is determined from the downstream equality in (2.14) i.e. setting

$$\frac{[j]}{[\tilde{u}]} = \left.\frac{\mathrm{d}j}{\mathrm{d}\tilde{u}}\right|_2, \tag{2.16}$$

which leads to $\tilde{u}_2 = \tilde{u}_{so} = 3/2k_2$. The construction in figure 2 also indicates that when sonic conditions hold the shock chord is tangential to the shock polar curve – a straightforward result to show. Inadmissible shocks then are associated with shock chords that cut the shock polar as seen for S_3.

The second important class of elementary solutions, aside from shocks, are simple waves – identified as flows associated with only one family of characteristics. Looking for solutions depending on only a single variable $r(\xi, \eta)$ i.e. $\tilde{u} = \tilde{u}(r)$, $\tilde{v} = \tilde{v}(r)$ we rewrite (2.3), (2.4) as

$$\frac{\mathrm{d}j}{\mathrm{d}r}\frac{\partial r}{\partial \xi} + \frac{\mathrm{d}\tilde{v}}{\mathrm{d}r}\frac{\partial r}{\partial \eta} = 0, \quad j = -K_1\tilde{u} - \tilde{u}^2 + \frac{K_2}{3}\tilde{u}^3, \tag{2.17a,b}$$

$$\frac{\mathrm{d}\tilde{u}}{\mathrm{d}r}\frac{\partial r}{\partial \eta}-\frac{\mathrm{d}\tilde{v}}{\mathrm{d}r}\frac{\partial r}{\partial \xi}=0. \tag{2.18}$$

Solutions for (r_ξ, r_η) exist then only if

$$\frac{\mathrm{d}\tilde{v}}{\mathrm{d}r}=\pm\sqrt{-\frac{\mathrm{d}j}{\mathrm{d}\tilde{u}}}\frac{\mathrm{d}\tilde{u}}{\mathrm{d}r}. \tag{2.19}$$

The curve $\tilde{u}(r)$, $\tilde{v}(r)$ parameterised by the 'phase' variable r has slope

$$\left.\frac{\mathrm{d}\tilde{v}}{\mathrm{d}\tilde{u}}\right|_r=\pm\left.\sqrt{-\frac{\mathrm{d}j}{\mathrm{d}\tilde{u}}}\right|_r \tag{2.20}$$

which is orthogonal to the straight line of constant phase given by

$$\left.\frac{\mathrm{d}\eta}{\mathrm{d}\xi}\right|_r=\mp\frac{1}{\sqrt{-\dfrac{\mathrm{d}j}{\mathrm{d}\tilde{u}}(r)}}, \tag{2.21}$$

which is the characteristic slope (compare with (2.13)). The similarity with (2.9) and (2.12) is clear. A relevant example of a simple wave is a centred wave fan with rays

$$\frac{\eta}{\xi}=\frac{1}{\sqrt{-\dfrac{\mathrm{d}j}{\mathrm{d}\tilde{u}}(r)}},\quad r_a\leqslant r\leqslant r_b, \tag{2.22}$$

which provides the continuous transition from one uniform flow $(\tilde{u}(r_a),\ \tilde{v}(r_a))$ to another uniform flow $(\tilde{u}(r_b), \tilde{v}(r_b))$ past sharp corners. Details of shock and wave fan constructions can be found in Kluwick & Cox (2018).

With these basic building blocks we can consider the problem of shock reflection. This problem has been the subject of extensive research in ideal gas dynamics with theoretical results going back to Mach (1878), Neumann (1963*a*), Neumann (1963*b*) and early experiments in Bleakney & Taub (1949). With the wedge angle measured by the parameter a we have for small angles the regular reflection pattern of figure 1. As is well known in the classical case $K_2 = 0$ with increasing angle a the shock reflection undergoes so-called irregular reflection off the channel wall. This involves the detachment of both the incident and reflected shock from the surface and the generation of a third and stronger shock which remains attached to the surface. The point at which the three shocks meet is termed the triple point (T). As indicated in figure 3 the flow also includes an expansion fan and a slip line (not drawn as not realisable in the irrotational flow model considered here). The inclusion of the wave fan is significant and helps resolve the so-called von Neumann paradox that three intersecting shocks are seen in experiments but unsupported by theoretical analysis. The inclusion of the wave fan is due to Guderley (1947), Guderley (1957) a result that was overlooked for many decades until recent work by Hunter & Brio (1997), Hunter & Brio (2000), Hunter & Tesdall (2004) on the unsteady transonic flow equations (the time-dependent form of equations (2.3) and (2.4) with $K_2 = 0$) and by Vasil'ev (1998) and Vasil'ev & Krajko (1999) for the compressible Euler equations. The structure in the neighbourhood of the triple point is complex and revealed in the numerical results of Tesdall & Hunter (2002) and Tesdall, Sanders & Popivanov (2015) and the

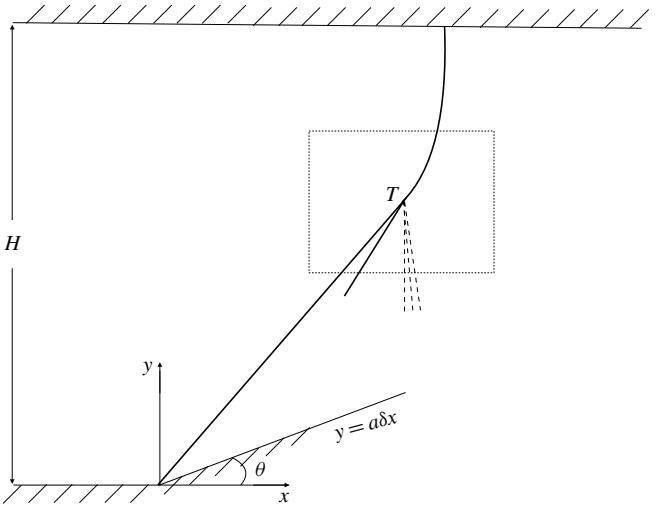

FIGURE 3. Flow geometry for irregular reflection of a plane shock generated by a wedge located at $x=0, y=0$ with inclination $a\delta>0$ in a channel of width H.

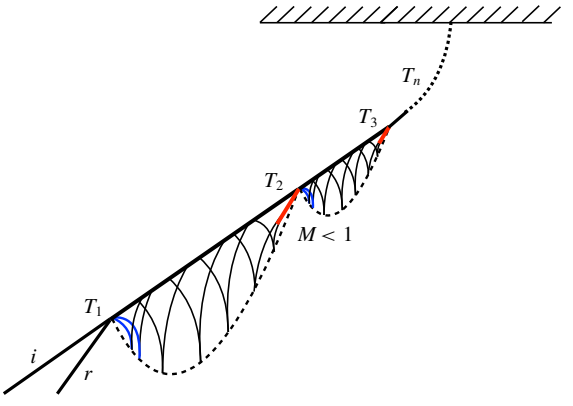

FIGURE 4. (Colour online) Sketch of the complex reflection structure due to Tesdall & Hunter (2002). Near the leading triple point T_1 there is a cascade of supersonic patches each patch terminated by a shock (in red) leading to multiple triple points $T_2, T_3 \ldots$. Blue lines denote centred wave fans generated at each triple point and dashed curves denote sonic curves bounding the supersonic patches.

experimental results of Cachucho & Skews (2012). These results are summarised in the sketch of figure 4. Behind the triple point $T=T_1$ of figure 3 there is a sequence of supersonic patches each patch terminated by a shock leading to multiple triple points $T_2, T_3 \ldots$.

In this paper we consider shock reflection for non-ideal gases using the modified small disturbance equations (2.3) and (2.4). In a previous paper (Kluwick & Cox 2018) the authors consider the flow over a ramp and in this follow-on paper we consider a shock generated by such a flow impinging now on a reflecting surface as encountered in a channel with a wedge.

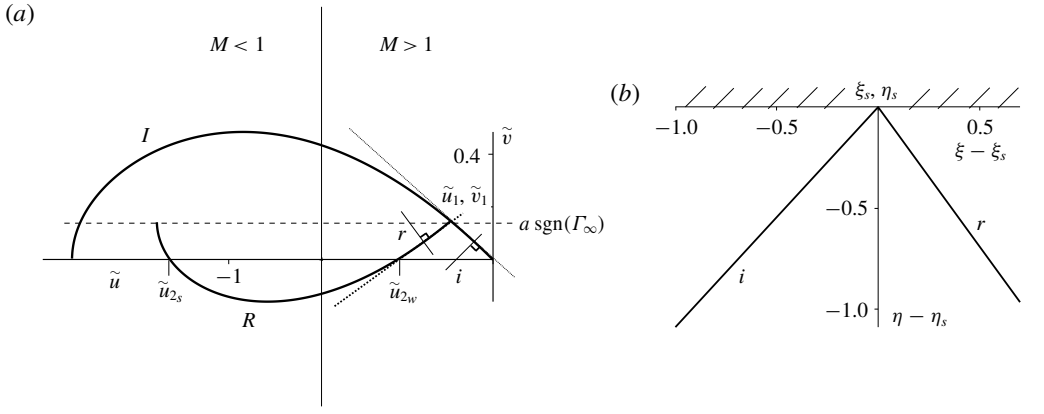

FIGURE 5. (*a*) Shock polars (incident polar I, reflected polar R) for regular reflection of a plane shock generated by a wedge with inclination a for $K_1 > 0$, $-3/4K_1 < K_2 \leqslant 0$. Results are for $K_1 = 1$, $K_2 = -0.7$. The incident shock i deflects the flow to $\tilde{u}_1$, $\tilde{v}_1$ and a weak reflected shock r generates supersonic flow $\tilde{u}_{2_w}$, $\tilde{v}_2 = 0$ downstream of the shock – flow which is parallel to the channel wall. The incident and reflected shocks are depicted in (*b*) in the (ξ, η) plane using the construction indicated in (*a*). The shock reflection point is labelled as (ξ_s, η_s).

3. Regular reflection

In Kluwick & Cox (2018) we identified distinctly different flows in the parameter space $(K_1 > 0, K_2)$ for the parameter ranges $K_2 < -1/K_1$, $-1/K_1 < K_2 < -3/4K_1$, $-3/4K_1 < K_2 \leqslant 0$ and $K_2 > 0$. For each of these intervals we now consider an incident shock reflection problem with the emphasis on regular reflection. We then show in § 4 that when regular reflection breaks down with increased ramp angle (or equivalently incident shock strength) the pure triple shock structure does not exist. This result extends a well-known result for ideal gases.

We note that descriptions of flows in this paper will assume that Γ_∞ is positive. This is to simplify the interpretation of the results obtained but is not a requirement for the analysis. As a consequence shocks are compressive and wave fans are expansive. The results are easily reinterpreted for an expanding channel with expansion shocks and compression wave fans associated with $\Gamma_\infty < 0$.

3.1. *Case:* $K_1 > 0$, $-3/4K_1 < K_2 \leqslant 0$

This case is qualitatively similar to the classical case which is included as a special case on setting $K_2 = 0$. The wave configuration for regular shock reflection is shown in figure 1 where a steady incident shock wave generated by a wedge reflects from a plane boundary. A reflected shock wave, formed at the point of intersection with the incident shock wave and the channel wall, then returns the flow which is deflected towards the wall by the incident shock to a flow parallel again to the wall.

The shock polars describing regular reflection are shown in figure 5(*a*) and represent the repeated application of (2.9) to the incident and reflected shocks. Without loss of generality we can assume that the upstream perturbed flow for the reflection problem is $\tilde{u} = 0$, $\tilde{v} = 0$. So the incident shock is described by possible downstream states $(\tilde{u}, \tilde{v})$ satisfying

$$\tilde{v}(\tilde{u}) = -\tilde{u}\sqrt{K_1 + \tilde{u} - \frac{K_2}{3}\tilde{u}^2}, \tag{3.1}$$

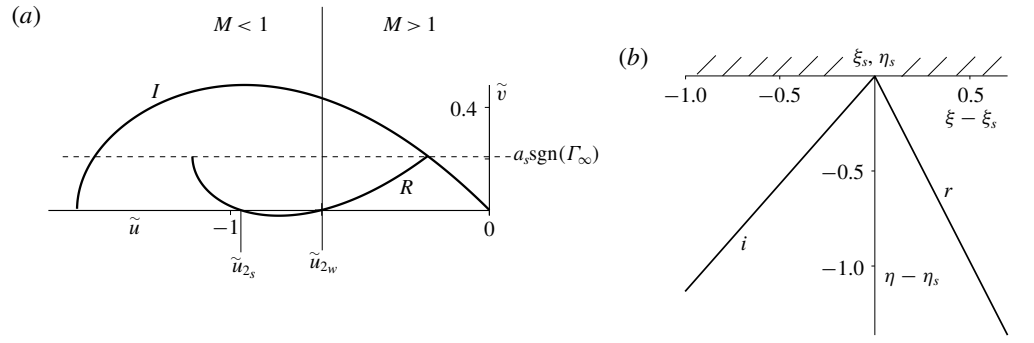

FIGURE 6. (*a*) Shock polar for regular reflection of a plane shock generated by a wedge with inclination a_s for $K_1 > 0, -3/4K_1 < K_2 \leqslant 0$. Results are for $K_1 = 1, K_2 = -0.7$. A weak reflected shock generates sonic flow $\tilde{u}_{2_w}, \tilde{v}_2 = 0$ which is parallel to the channel wall. The incident (*i*) and reflected shock (*r*) are depicted in (*b*). The shock reflection point is labelled as (ξ_s, η_s).

and plotted as curve I in figure 5(*a*). A wedge inclination angle of magnitude a generates, as shown, two possible downstream flows satisfying the wedge boundary condition $\tilde{v} = a$ sign Γ_∞, see (2.8*b*). We will consider a weak incident shock jump to a supersonic state $\tilde{u}_1$, $\tilde{v}_1 = a$ sign Γ_∞ located on the incident shock polar I in figure 5(*a*).

The reflected shock then is described by downstream states $(\tilde{u}_2, \tilde{v}_2)$ with states $(\tilde{u}_1, \tilde{v}_1)$ upstream. This reflected shock polar derived from (2.9) is given by

$$\tilde{v}_2(\tilde{u}_2) = \tilde{v}_1 + (\tilde{u}_2 - \tilde{u}_1)\sqrt{K_1 + \tilde{u}_1 + \tilde{u}_2 - \frac{K_2}{3}(\tilde{u}_1^2 + \tilde{u}_2^2 + \tilde{u}_1\tilde{u}_2)}. \tag{3.2}$$

The reflected shock polar R intersects the $\tilde{v} = 0$ axis at two values of $\tilde{u}_2$ both corresponding to possible downstream flow states. We distinguish these two downstream states as in one case generating a weak shock connecting typically to supersonic flow downstream $(\tilde{u}_{2_w}, \tilde{v}_2 = 0)$ and in the other case generating a strong shock connecting always to a subsonic flow downstream $(\tilde{u}_{2_s}, \tilde{v}_2 = 0)$. Which state is realised in practice depends critically on the boundary conditions downstream and the reader is encouraged to see the discussion in Kluwick & Cox (2018) for more details. It is the weak shock certainly that is commonly observed in experiments and depicted in figure 5. The incident and reflected shocks have slopes given by (2.12) and are plotted in figure 5(*b*) in the asymptotic coordinate system (ξ, η). We have indicated in figure 5(*a*) the construction leading to the determination of the shock slopes in figure 5(*b*) which implements (2.12).

The regular reflection pattern shown in figure 5 holds for small wedge inclination angles. As the wedge angle is increased the weak downstream shock state associated with the reflected shock eventually becomes sonic with $M = 1$. The value of a at which this occurs is denoted by a_s. The shock polars for this case are shown in figure 6(*a*) and the incident and reflected shocks in the (ξ, η) plane are shown in figure 6(*b*). With increasing $a > a_s$ the weak shock now describes a jump to subsonic downstream states as shown in figure 7 and with further increases in wedge angle a eventually the weak and strong downstream states coalesce. This gives a detachment wedge angle $a = a_d$ such that for values of $a > a_d$ regular reflection becomes impossible. For $a > a_d$ the

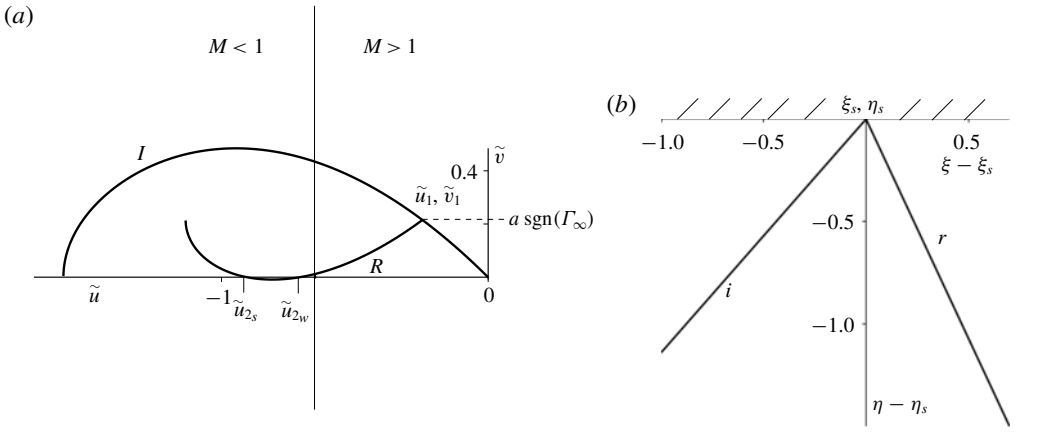

FIGURE 7. (*a*) Shock polar for regular reflection of a plane shock generated by a wedge with inclination $a > a_s$ for $K_1 > 0$, $-3/4K_1 < K_2 \leqslant 0$. Results are for $K_1 = 1$, $K_2 = -0.7$. The incident shock I deflects the flow to $\tilde{u}_1$, $\tilde{v}_1$ and a weak reflected shock generates subsonic flow $\tilde{u}_{2_w}$, $\tilde{v}_2 = 0$ which is parallel to the channel wall. The incident and reflected shocks are depicted in (*b*). The shock reflection point is labelled as (ξ_s, η_s).

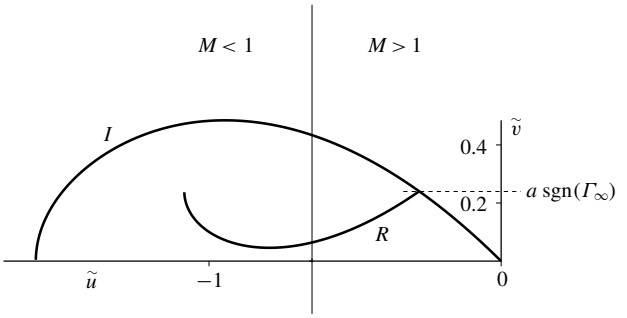

FIGURE 8. Shock polar for reflection of a plane shock generated by a wedge with inclination $a > a_d$ for $K_1 > 0$, $-3/4K_1 < K_2 \leqslant 0$. Results are for $K_1 = 1$, $K_2 = -0.7$. No reflected shock can return the fluid flow to downstream parallel channel flow.

flow after any reflected shock is still positive towards the wall and the downstream $\tilde{v} = 0$ boundary condition cannot be satisfied by any point on the reflected shock polar, see figure 8.

It is possible in the ideal gas case ($K_2 = 0$) to evaluate a_s and a_d explicitly and a straightforward calculation gives

$$a_s = \frac{(3-\sqrt{5})\sqrt{1+\sqrt{5}}}{8} K_1^{3/2} \approx 0.1718 K_1^{3/2}, \quad a_d = \frac{2}{5^{3/2}} K_1^{3/2} \approx 0.1789 K_1^{3/2}. \quad (3.3a,b)$$

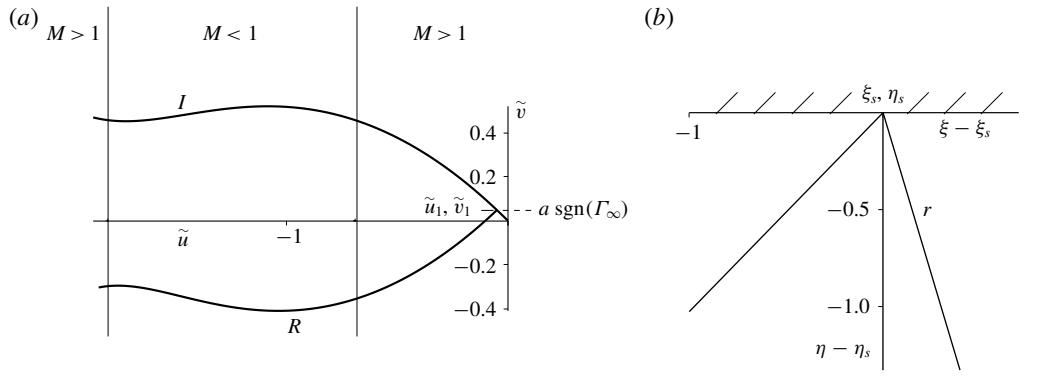

FIGURE 9. (*a*) Shock polar for regular reflection of a plane shock generated by a wedge with inclination a for $K_1 > 0$, $-1/K_1 < K_2 < -3/4K_1$. Results are for $K_1 = 1$, $K_2 = -0.8$. The incident shock generated on the incident shock polar I deflects the flow to $\tilde{u}_1$, $\tilde{v}_1$ with $\tilde{u}_1 = -0.05$ and a reflected supersonic shock returns the flow parallel to the channel wall. The incident shock (i) and reflected sonic shock (r) are depicted in (*b*). The shock reflection point is at (ξ_s, η_s).

3.2. *Case:* $K_1 > 0$, $-1/K_1 < K_2 < -3/4K_1$

In the previous case the shock reflection problem led to flows similar to the classical case with $\Lambda_\infty = 0$ ($K_2 = 0$). With decreasing values of K_2 and so larger negative values of Λ_∞ the shock reflection problem begins to show features that have no counterpart in ideal gas dynamics.

For small wedge angles the incident and reflected shock polar plots are given in figure 9(*a*) for $\tilde{u}_1 = -0.05$, $K_1 = 1$ and $K_2 = -0.8$. The construction is as already described in the previous case in § 3.1. The polar plots terminate now not with normal orientated shocks but with sonic conditions, i.e. shocks of increased strength would result in the shock chord cutting the shock polar – these are excluded. It is clear that the reflected shock polar intersects the $\tilde{v} = 0$ axes now only once to give a unique reflection shock with a supersonic downstream state returning the deflected flow to parallel channel flow. With increasing wedge angle we have a three shock solution shown in figure 10 involving now an additional subsonic downstream flow labelled $\tilde{u}_3$ as well as the two-shock solution similar to the classical ideal gas reflections.

As the wedge angle continues to increase the flow scenarios associated with the reflected shock jumps to $\tilde{u}_3$ become more complicated as shown in the reflected shock polar plots of figure 11 which should be compared to the inset in figure 10. The downstream state $\tilde{u}_3$ with increasing angle (i.e. decreasing $\tilde{u}_1$) eventually becomes supersonic and then with further increases the reflected shock is a downstream sonic shock and shock state $\tilde{u}_3$ is replaced by a sonic shock to $\tilde{u}_{so}$ and a centred fan structure returning the flow to parallel channel flow. This latter scenario is shown in figure 12(*a*) for $\tilde{u}_1 = -0.13185$ with the three possible reflection flows one of which is the compound shock/fan structure. The centred wave fan is constructed from (2.20) (with the appropriate sign) which we integrate from $(\tilde{u}_{so}, \tilde{v}_{so})$ to $(\tilde{u}_3, 0)$. In figure 12(*b*) the reflected sonic shock r and the attached wave fan rays terminating at $\tilde{u}_3$ are plotted for this latter case where we have used the shock slope condition (2.12) and the characteristic ray equation (2.22).

Shock behaviour described by figure 12 does not persist as the wedge angle continues to increase. The compound downstream shock/wave fan structure requires

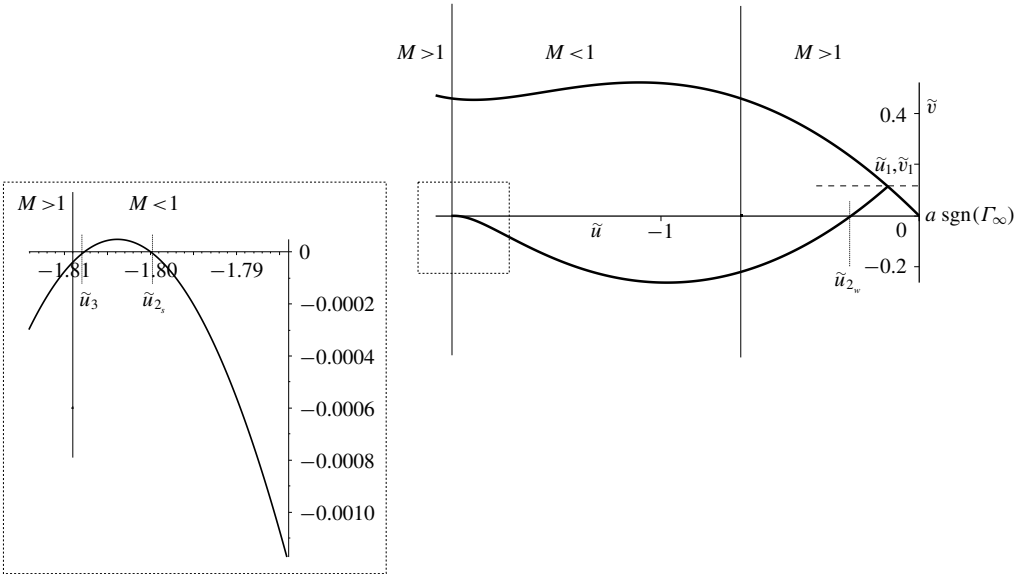

FIGURE 10. Shock polar for regular reflection of a plane shock generated by a wedge with inclination a for $K_1 > 0$, $-1/K_1 < K_2 < -3/4K_1$. Results are for $K_1 = 1$, $K_2 = -0.8$. The incident shock generated on the incident shock polar I deflects the flow to $\tilde{u}_1, \tilde{v}_1$ with $\tilde{u}_1 = -0.12175$. Reflection shocks are possible to three downstream states a weak shock $\tilde{u}_{2_w}$ and as included in the inset two strong subsonic shock states $\tilde{u}_{2_s}$ and $\tilde{u}_3$.

that the sonic shock involves a jump transition to supersonic flow downstream. A shock bifurcation occurs when the wedge angle increases so that the incident shock involves a jump to

$$\tilde{u}_1 = \frac{1 - 2\sqrt{1 + K_1 K_2}}{K_2}. \tag{3.4}$$

At this point the reflected sonic shock is normal to the channel wall and describes a jump to sonic ($M = 1$) downstream flow. The shock polar plot for this bifurcating flow is shown in figure 13. For increasing wedge angles so that $\tilde{u}_1 < (1 - 2\sqrt{1 + K_1 K_2})/K_2$ the compound shock/fan flow is now no longer possible and the shock polars describe a classical reflection pattern involving the transition, with increasing wedge angle, from a strong subsonic and weak supersonic reflected shock to two subsonic reflected shocks as shown by the shock polar curves in figure 14 for $\tilde{u}_1 = -0.257$.

Non-classical behaviour involving a compound sonic shock/wave fan occurs over a narrow range of incident shock strengths (or wedge angles). For the particular flow described with $K_1 = 1$ and $K_2 = -0.8$ the existence of a third solution branch occurs in the interval

$$-0.131966 \lesssim \tilde{u}_1 \lesssim -0.1217425. \tag{3.5}$$

3.3. *Case:* $K_1 > 0, K_2 < -1/K_1$

In the previous cases the shock reflection problem has multiple solutions. In contrast the shock configuration is unique for $K_2 < -1/K_1$. We will consider

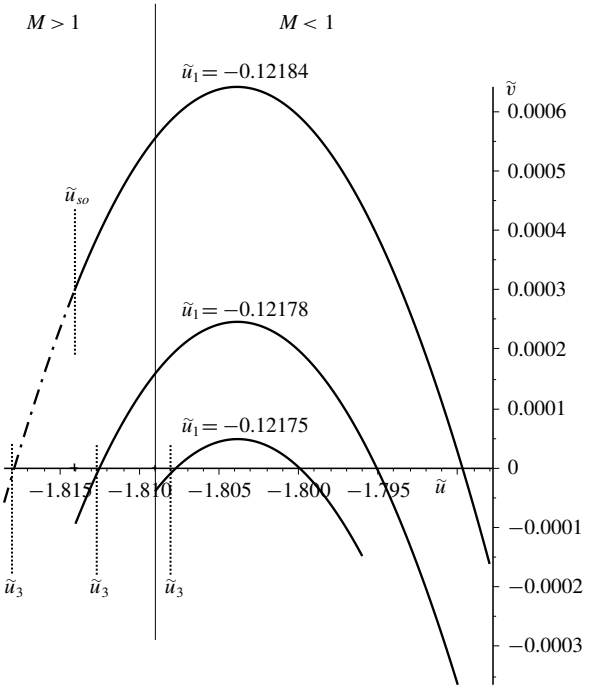

FIGURE 11. Section of reflection polar $K_1 > 0$, $-1/K_1 < K_2 < -3/4K_1$. Results are for $K_1 = 1, K_2 = -0.8$. The transition is shown to a compound shock/fan structure as the wedge angle increases (or $\tilde{u}_1$ decreases) leading to the downstream state $\tilde{u}_3$.

values of a less than

$$a \operatorname{sign} \Gamma_\infty = -\frac{3}{2K_2}\sqrt{K_1 + \frac{3}{4K_2}}, \tag{3.6}$$

which is the wedge angle, as shown in figure 15, at which an incident shock becomes sonic and beyond which the incident flow consists of a compound sonic shock/wave fan structure. We have for small wedge angles a classical regular reflection shock configuration as seen in figure 15. With increasing wedge angle the reflected shock consists of a sonic shock/wave fan configuration and as the wedge angle increases further the reflected shock strength decreases until with a greater than

$$a \operatorname{sign} \Gamma_\infty = -\frac{1}{K_2}\sqrt{K_1 + \frac{2}{3K_2}}, \tag{3.7}$$

the incident shock generates a reflected wave fan only. The analysis used to plot figure 15 is that already described in §§ 3.1 and 3.2.

3.4. *Case:* $K_1 > 0, K_2 > 0$

From a careful reading of Kluwick & Cox (2018) the only relevant flow is associated with negative downstream $\tilde{u}$ values. The shock polars are qualitatively similar to the classical case and the reflection problem can be analysed in a similar manner. We do not provide details of this case.

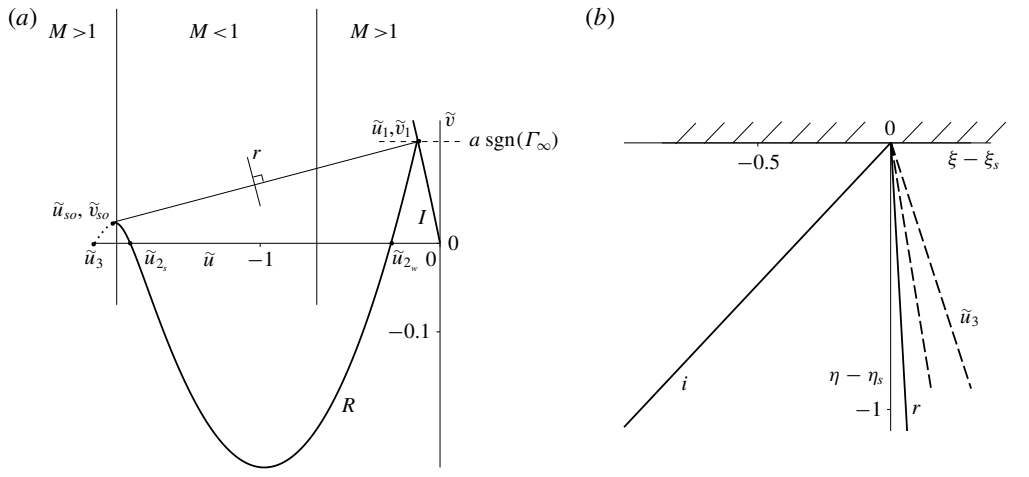

FIGURE 12. (*a*) Shock polar for regular reflection of a plane shock generated by a wedge with inclination a for $K_1 > 0$, $-1/K_1 < K_2 < -3/4K_1$. Results are for $K_1 = 1$, $K_2 = -0.8$. The incident shock generated on the incident shock polar I deflects the flow to $\tilde{u}_1$, $\tilde{v}_1$ with $\tilde{u}_1 = -0.13185$. Reflection shocks are possible to three downstream states a weak shock $\tilde{u}_{2_w}$ a strong subsonic shock $\tilde{u}_{2_s}$ and a compound sonic shock $\tilde{u}_{so}$ and wave fan to $\tilde{u}_3$. The sonic shock (r) and rays for the attached fan are shown in (*b*).

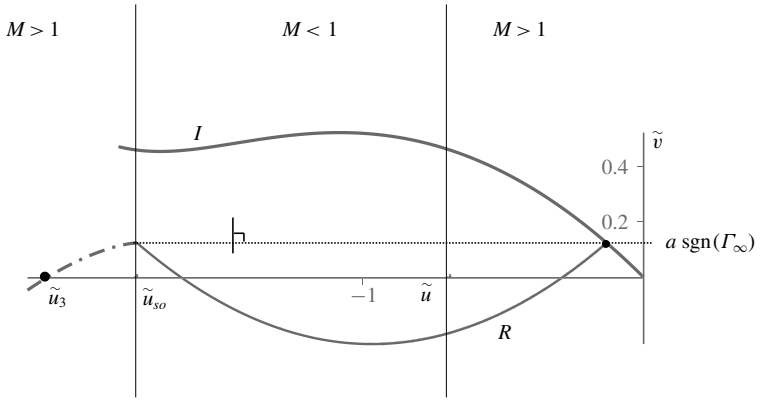

FIGURE 13. Shock polar for strong reflected shocks for $K_1 > 0$, $-1/K_1 < K_2 < -3/4K_1$. Results are for $K_1 = 1$, $K_2 = -0.8$. A non-classical reflection shock/fan solution is obtained for $\tilde{u}_1 = (1 - 2\sqrt{1 + K_1 K_2})/K_2$ involving a normal orientated sonic reflection shock and an attached fan with a transition to $\tilde{u}_3$ downstream.

4. Irregular reflection

It is a well-known result that in planar steady flows a pure triple shock structure does not exist i.e. you cannot have three shocks intersecting with constants states between them. This result is discussed, for example, in Courant & Friedrichs (1948), Neumann (1963*a*), Neumann (1963*b*) and Henderson & Menikoff (1998). More recently in Serre (2007) a proof is presented that is independent of any

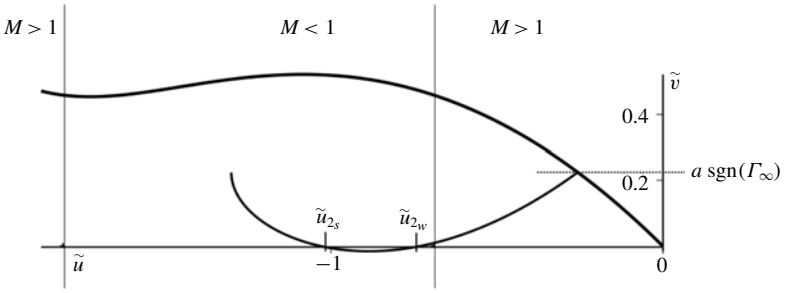

FIGURE 14. Shock polar for $K_1 > 0$, $-1/K_1 < K_2 < -3/4K_1$. Results are for $K_1 = 1$, $K_2 = -0.8$. Two classical subsonic solutions $\tilde{u}_{2_w}$ and $\tilde{u}_{2_s}$ are obtained for $\tilde{u}_1 = -0.257$.

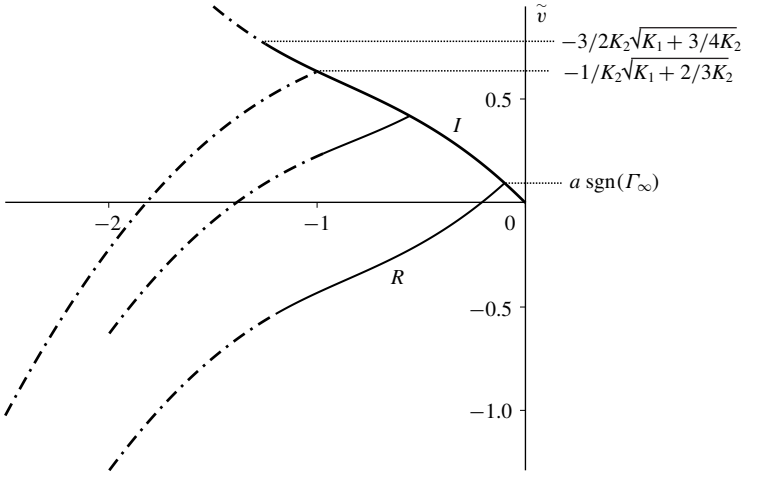

FIGURE 15. Shock polar for regular reflection of a plane shock generated by a wedge with inclination a for $K_1 > 0$, $K_2 < -1/K_1$. Results are for $K_1 = 1$, $K_2 = -1.2$. Small wedge angles lead to a classical regular reflection shock. Larger wedge angles lead to a sonic shock/wave fan configuration. Wedge angles with a greater than $a\ \mathrm{sign}\ \Gamma_\infty = -(1/K_2)\sqrt{K_1 + 2/3K_2}$ result in a reflected wave fan only.

assumption on the equation of state of the gas. A corresponding result for the unsteady transonic small disturbance equation can be found in Tabak & Rosales (1994). The result presented here is for steady flow of the modified transonic small disturbance equation and is based on the geometry of the shock polar curves. In figure 16(*a*) we show the shock geometry associated with a pure triple shock with the reflected shock (r) and incident shock (i) both forward facing. Both shocks intersect a third shock – the so-called Mach stem (m) at the triple point (T). In figure 16(*b*) we show the plot of the reflected polar when $a > a_d$ as illustrated for K_2 in the parameter range $-3/4K_1 < K_2 < 0$. A shock from state $(\tilde{u}_1 = 0, \tilde{v}_1 = 0)$ to state $(\tilde{u}_2, \tilde{v}_2)$ on the incident shock polar is followed by a second shock from $(\tilde{u}_2, \tilde{v}_2)$ to $(\tilde{u}_3, \tilde{v}_3)$ where $(\tilde{u}_3, \tilde{v}_3)$ lies on the reflected shock polar. The requirement that a triple shock arrangement is possible would require that the reflected shock polar intersects the incident shock polar at $(\tilde{u}_3, \tilde{v}_3)$ generating a third jump from (0, 0) to $(\tilde{u}_3, \tilde{v}_3)$.

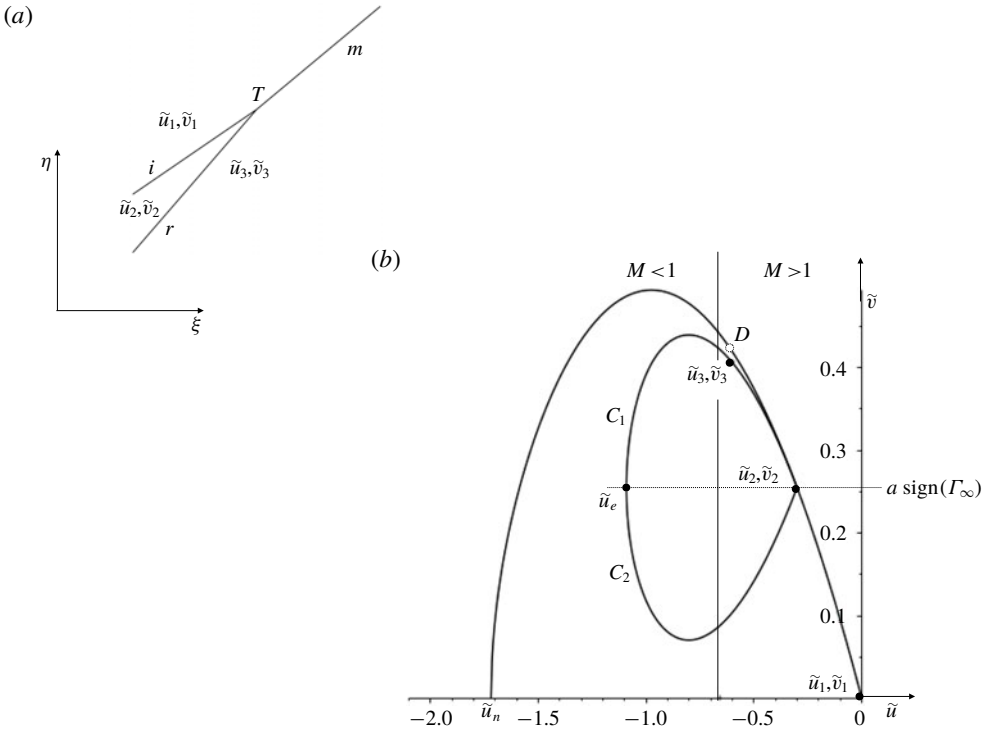

FIGURE 16. (*a*) Sketch of the shock geometry in the ξ, η plane associated with a pure triple point construction. The incident shock (i), reflected shock (r) and Mach stem (m) intersect at the triple point (T). (*b*) Shock polars for irregular reflection of a plane shock generated by a wedge with inclination $a > a_d$ for $K_1 > 0$, $3/4K_1 < K_2 < 0$. The incident shock i deflects the flow to $\tilde{u}_2$, $\tilde{v}_2$ and a weak reflected shock (r) generates supersonic flow $\tilde{u}_3$, $\tilde{v}_3$. The pure triple point construction in (*a*) would require that $\tilde{u}_3$, $\tilde{v}_3$ coincides with the point D on the incident shock polar.

This does not occur as seen in figure 16(*b*) – a result that we can prove holds more generally.

The incident shock polar for $(\tilde{u_1} = 0, \tilde{v_1} = 0)$ is given by the curve

$$\tilde{v}(\tilde{u}) = -\tilde{u}\sqrt{K_1 + \tilde{u} - \frac{K_2}{3}\tilde{u}^2}, \quad \tilde{u}_n \leqslant \tilde{u} < 0, \tag{4.1}$$

which gives all flow states $(\tilde{u}, \tilde{v}(\tilde{u}))$ that can be connected to $(0, 0)$ by an incident shock. For a given state $\tilde{v}_2 = \tilde{v}(\tilde{u}_2)$ we construct then the reflected shock polar which describes all flows which can be connected to $(\tilde{u_2}, \tilde{v_2})$ by a reflected shock. These are the flow states

$$\tilde{v}(\tilde{u}) = -\tilde{u_2}\sqrt{K_1 + \tilde{u_2} - \frac{K_2}{3}\tilde{u_2}^2} - (\tilde{u} - \tilde{u_2})\sqrt{K_1 + \tilde{u} + \tilde{u_2} - \frac{K_2}{3}(\tilde{u}^2 + \tilde{u}\tilde{u}_2 + \tilde{u}_2^2)},$$
$$\tilde{u}_e \leqslant \tilde{u} < \tilde{u}_2, \tag{4.2}$$

and depicted as the labelled curve C_1 in figure 16(*b*). We have assumed here that the reflected shock is a forward pointing shock. Now we require that the incident shock

curve given by (4.1) lies above the reflected shock curve (4.2). It is readily shown that this reduces to the inequality

$$\sqrt{K_1+\tilde{u}-\frac{K_2}{3}\tilde{u}^2}<\sqrt{K_1+\tilde{u}_2-\frac{K_2}{3}\tilde{u}_2^2},\quad \tilde{u}_e\leqslant\tilde{u}<\tilde{u}_2, \tag{4.3}$$

which is true providing

$$1-\frac{K_2}{3}(\tilde{u}+\tilde{u}_2)>0. \tag{4.4}$$

This inequality which is trivially true for $K_2=0$ holds in the two cases $-1/K_1<K_2<-3/4K_1$ and $-3/4K_1<K_2\leqslant 0$ where we can show that

$$1-\frac{K_2}{3}(\tilde{u}+\tilde{u}_2)>\frac{1}{3}. \tag{4.5}$$

For the remaining $K_2>0$ case as we require that that the flow downstream of the incident shock is supersonic this excludes sonic incident shocks. The remaining flows have $\tilde{u}+\tilde{u}_2<0$ and so inequality (4.4) is trivially satisfied.

An important consequence of this result is the von Neumann paradox. For ideal gases numerical results and experiments show that for certain parameters the fluid flow appears to be described by three shocks separated by constant states which contradicts the theoretical results. A resolution of this paradox is the scenario given by Tesdall & Hunter (2002), Tesdall *et al.* (2015) where numerical experiments on a fine grid show that there is a supersonic region behind the triple point, which consists of a sequence of supersonic patches, shocks, wave fans and multiple triple points. The numerical results do not indicate whether there are finitely many such triple points or not.

We can provide analysis that suggests a similar construction holds in the dense gas case. Hunter & Brio (2000) proposed the shock configuration shown in figure 3 where as well as an incident shock, reflected shock and Mach stem there is a centred simple wave behind the reflected shock. The incident, reflected and Mach shocks are all forward facing and the wave fan is backward facing. Given the upstream state ($\tilde{u}=0$, $\tilde{v}=0$), the wedge angle a and the flow behind the reflected shock $\tilde{u}_2$ this configuration can be uniquely constructed. An argument presented in Guderley (1957) suggests that the flow behind the reflected shock is sonic. This leads to the shock polar/characteristic construction shown in figure 17 for the case $K_2>0$ and $-3/4K_1<K_2<0$. The expansion fan is generated by the characteristic curve obtained by integrating

$$\frac{\mathrm{d}\tilde{v}}{\mathrm{d}\tilde{u}}=\sqrt{K_1+2\tilde{u}-K_2\tilde{u}^2}, \tag{4.6}$$

from the sonic state $\tilde{u}=\tilde{u}_3=(1/K_2)(1-\sqrt{1+K_1K_2})$ to $\tilde{u}=\tilde{u}_4$ where the characteristic curve (4.6) intersects the incident shock polar. While (4.6) can be integrated analytically the point of intersection with the incident shock has to be determined numerically. Figure 17(*b*) shows the shock and wave fan orientations and the flow deflected through the Mach stem (*m*). The flow downstream of the Mach stem is still not aligned with the channel wall and so cannot describe the full reflection problem which must certainly involve a curved Mach stem eventually orientated to generate a normal shock at the channel wall. The likely solution is that proposed by Tesdall & Hunter (2002) where the expansion fan reflects off a sonic curve to form a compression wave which in turn generates a shock that incident on the Mach stem generates a new expansion fan. This process can be repeated with a shrinking series

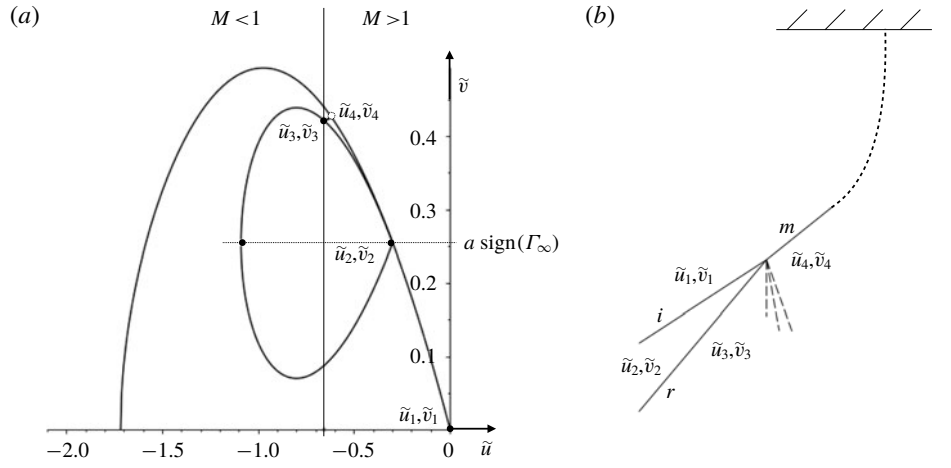

FIGURE 17. (*a*) Shock polar and characteristic plot for irregular reflection of a plane shock generated by a wedge with inclination a for $K_1 > 0$, $-3/4K_1 < K_2 \leqslant 0$. Results are for $K_1 = 1$, $K_2 = -0.73$. The incident shock i deflects the flow to $\tilde{u}_2$, $\tilde{v}_2$ and a weak reflected shock (r) generates the sonic flow $\tilde{u}_3$, $\tilde{v}_3$ downstream. A centred wave fan solution describes a continuous expansion from $\tilde{u}_3$, $\tilde{v}_3$ to $\tilde{u}_4$, $\tilde{v}_4$ which intersects the incident shock polar and generates the shock jump across the Mach stem (m). This so-called Guderley reflection is plotted in (*b*) with a sketch appended (dotted line) of the curved Mach stem that then returns the flow to parallel downstream channel flow.

of supersonic pockets generated as sketched in figure 4. The recent high resolution results of Tesdall *et al.* (2015) confirms this picture for ideal gases.

The scenario of a curved Mach stem orientating the flow to normal channel flow at the boundary has to be modified for the case $-1/K_1 < K_2 < -3/4K_1$. Observations are based on the shock polar diagram of figure 18. As the Mach stem shock originating at $\tilde{u}_4$, $\tilde{v}_4$ increases in strength the flow downstream becomes supersonic and eventually the Mach stem shock turns sonic with downstream flow $\tilde{u}_{so}$. The Mach stem shock remains sonic (and so of fixed orientation) with then decreasing downstream $\tilde{v}$ values now associated with a wave fan along the characteristic curve (dash-dot curve) connecting $\tilde{u}_{so}$ to $\tilde{u}_e$. This wave fan propagates into a subsonic downstream region and will itself form a supersonic pocket by reflection from a sonic boundary. A possible flow pattern is sketched in figure 19 where we note that as for the triple point the wave fan characteristics reflecting off the sonic curve are expected to intersect constructing a new downstream shock. Current research is underway to confirm this proposed scenario.

5. Conclusions

The analysis of Kluwick & Cox (2018) is extended to treat the problem of weak shock reflection in a channel. Together with the results derived in Kluwick & Cox (2018) the present work yields a complete picture of dense gas transonic flow past a configuration frequently used in wind tunnel experiments which also represents a simple model of the entry region of a gas turbine designed to exploit possible advantages such as increased efficiency resulting from the use of gases with high molecular complexity.

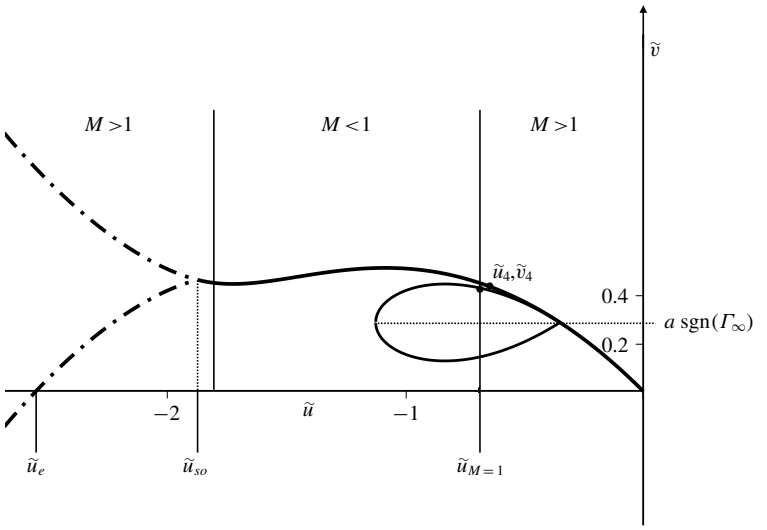

FIGURE 18. Shock polar plot for irregular reflection of a plane shock generated by a wedge with inclination a for $K_1 > 0$, $-1/K_1 < K_2 < -3/4K_1$. Results are for $K_1 = 1$, $K_2 = -0.8$. A proposed curved Mach stem is generated from the shock polar connecting the downstream state $(\tilde{u}_4, \tilde{v}_4)$ to $\tilde{u}_{so}$ where the Mach stem shock becomes sonic. Flow described by a characteristic (dash-dot) curve returns the flow through a wave fan to normal orientated channel flow on the boundary with $\tilde{u} = \tilde{u}_e$.

To study non-classical gas dynamic effects associated with such flow media analytically we assume transonic flow $|M_\infty - 1| \ll 1$ and $|\Gamma_\infty| \ll 1$ while the quantity $\Lambda(\rho, s) = \rho(\partial\Gamma/\partial\rho)|_s$ is taken to be of $O(1)$. It is then found that solutions of the problem under consideration depend on the elements of the non-dimensional group (a, K_1, K_2) representing, respectively, the strength of the incident shock generated by a ramp with ramp angle a, a generalised transonic similarity parameter and the combined effects of Γ_∞ and Λ_∞. As in classical gas dynamics, two essentially different classes of solutions classified as regular and irregular reflections have to be distinguished.

Flow patterns of the first type are characterised by the property that there exists a reflected shock or a compound shock/wave structure which emanates from the point where the incident shock impinges at the upper channel wall and returns the thereby deflected flow to a flow parallel to the wall again. Consequently, the reflected wave pattern is self-similar and can be constructed by appropriate generalisations of methods introduced in Kluwick & Cox (2018) to study the ramp problem. For upstream supersonic flow $K_1 > 0$ considered here three ranges of the second similarity parameter K_2 corresponding to qualitatively different flow scenarios can be identified. For negative values of K_2 larger than $-3/4K_1$ the flow behaviour is similar to the one known from classical gas dynamics, which is included as the special case $K_2 = 0$. In the two remaining distinguished parameter ranges $-1/K_1 < K_2 < -3/4K_1$ and $K_2 < -1/K_1$ the resulting flow pattern, however, exhibits features which have no counterpart in ideal gas dynamics.

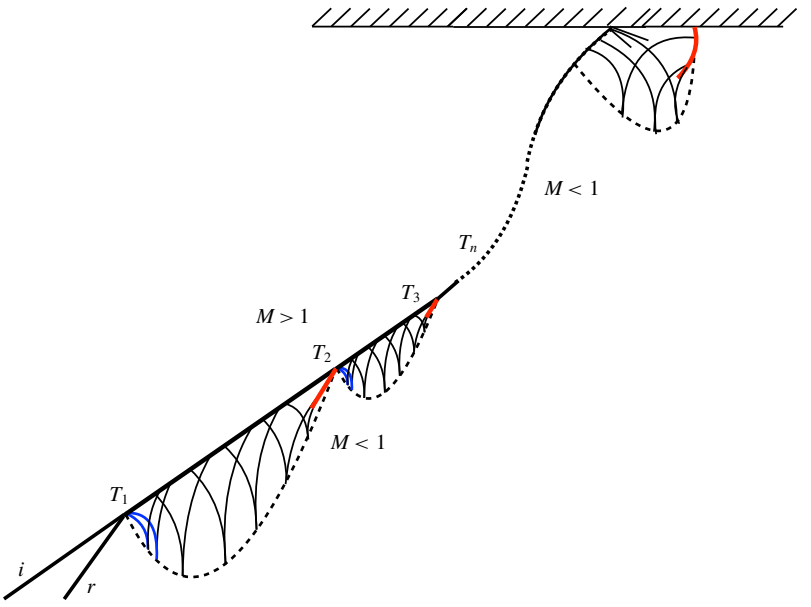

FIGURE 19. (Colour online) Sketch of flow scenario associated with a sonic Mach stem generating a supersonic pocket attached to the reflecting channel wall and terminating in an upstream shock.

Parameter range	Flow response
$-\frac{3}{4K_1} < K_2 < 0$	Two solutions representing weak and strong reflection (figures 5, 6, 7)
$-\frac{1}{K_1} < K_2 < -\frac{3}{4K_1}$	Up to 4 different solutions including non-classical phenomena such as sonic shocks and compound shock/fan structures (figures 9, 10, 11, 12, 13) but also cases of weak and strong reflection (figure 14)
$K_2 < -\frac{1}{K_1}$	Unique solutions. Increasing ramp angles cause the transition from a classical regular reflected shock to a sonic shock/fan combination and finally to the truly exotic situation of a pure reflected fan (figure 15)

TABLE 1. Overview of the phenomena observed for $K_2 < 0$.

Table 1 is intended to provide a more detailed but still compact overview of the phenomena observed for $K_2 < 0$.

With increasing ramp angle the point of shock reflection eventually is found to detach from the upper wall if a critical value a_{crit} is exceeded. In such cases of irregular reflection self-similarity of the associated wave pattern is lost which makes the analytical treatment of the full problem impossible although analytical progress is still possible by seeking local solutions. Experiments for perfect gases suggest the existence of a triple point formed by three colliding shocks: the incident and the reflected shocks and the Mach stem which extends up to the solid wall to satisfy the boundary condition there. Theoretical analysis for perfect as well as arbitrary media,

however, predicts that a pure triple shock configuration, i.e. three shocks separated by regions of constant state, is impossible, (Courant & Friedrichs 1948; Neumann 1963*a*,*b*; Henderson & Menikoff 1998; Serre 2007). The present analysis shows that this result, known as the von Neumann paradox, is consistently captured by the transonic flow approximation for the type of fluids which are of interest here: the reflected shock polar for values $a > a_{crit}$ is located completely inside the incident shock polar. Therefore, both polars do not intersect and consequently there is no common state downstream of the Mach stem and the reflected shock. To the authors' knowledge this graphical interpretation of the von Neumann paradox has been pointed out first by Oswatitsch (1977) for perfect gases but is non-trivially extended even to cases of dense gases where the incident shock polar in the hodograph plane is no longer closed but terminates if sonic conditions are reached and thus has to be supplemented with characteristic curves which emanate from the point where the shock polar terminates. As for perfect gases one possibility to resolve the von Neumann paradox in the context of transonic flows is that proposed by Guderley as early as 1957 but which did not receive full recognition until recently. Guderley argued that the state behind the reflected shock is sonic and connects with the state downstream of the Mach stem via a weak wave fan. It should be noted that the resulting four wave system formed by the incident shock, the reflected shock, the Mach stem and the intervening wave fan represents an exact solution of the transonic small perturbation equation for both perfect and dense gases. However, it does not satisfy the boundary condition at the upper channel wall and thus, as far as the global flow field is concerned, has to be interpreted as a solution which describes the local flow behaviour close to the origin of the wave fan confined within a small supersonic pocket. Recent numerical solutions, see Tesdall *et al.* (2015) and references therein, indicate that this pocket spawns additional local supersonic patches. A possible explanation is based on observations known from conventional aerodynamics, that local supersonic regions in general generate shocks which, in the present context, then provide the agents to perpetuate the mechanism introduced to eliminate the von Neumann paradox in the first place. It is therefore expected that irregular reflections in dense gases will be qualitatively similar to those in perfect gases. A new non-classical feature, however, arises in cases where the shock polar in the hodograph plane is no longer closed but terminates at a sonic point with the normal velocity component v being non-zero. Consequently, the interaction of a single Mach stem shock with the upper wall is not able to satisfy the boundary condition $v = 0$ there. Rather the combined action of an oblique Mach stem shock with an attached wave fan is required to return the deflected flow to a flow again parallel to the wall. Numerical work to support this tentative picture is presently been carried out.

The present analysis is based on the assumption of inviscid strictly two-dimensional flow. Extensions to represent the dynamics of more 'realistic' flows are clearly desirable. Questions concerning the stability of solutions involving shocks have been addressed already in Kluwick & Cox (2018) and will not be repeated here. Following the study by Kluwick & Kornfeld (2014) weakly three-dimensional effects can in principle be incorporated by letting the various flow quantities depend on an additional Cartesian coordinate which varies slowly in the lateral direction. Triple-deck theory is expected to provide the proper framework to account for the effects of laminar boundary layers in the limit of high Reynolds number, (Wrabel & Kluwick 2005; Kluwick & Meyer 2010, 2011). Here the differences of the flow field caused by compression shocks which drive the flow towards separation and rarefaction shocks

which accelerate the flow medium will be of prime interest. First steps in the treatment of fully developed turbulent dense gas in unconfined and channel flows in have been taken by Alferez & Touber (2017), Sciacovelli, Cinnella & Gloerfelt (2017). Further progress in the treatment of aerodynamic configurations will require the formulation of a strategy based on the Reynolds averaged equations, see e.g. Walker (1998).

REFERENCES

ALFEREZ, N. & TOUBER, E. 2017 One-dimensional refraction properties of compression shocks in non-ideal gases. *J. Fluid Mech.* **814**, 185–221.

BECKER, R. 1922 Stosswelle und Detonation. *Z. Phys.* **8** (1), 321–362.

BETHE, H. A. 1942 The theory of shock waves for an arbitrary equation of state. Technical paper 545, Office Sci. Res. & Dev.

BLEAKNEY, W. & TAUB, A. H. 1949 Interaction of shock waves. *Rev. Mod. Phys.* **21**, 584–605.

CACHUCHO, A. & SKEWS, B. W. 2012 Guderley reflection for higher Mach numbers in a standard shock tube. *Shock Waves* **22** (2), 141–149.

CINELLA, P. & CONGEDO, P. M. 2005 Aerodynamic performance of transonic Bethe–Zel'dovich–Thompson flows past an airfoil. *AIAA J.* **43**, 370–378.

COLE, J. D. & COOK, P. 1986 *Transonic Aerodynamics*. Elsevier.

CONGEDO, P. M., CORRE, C. & CINELLA, P. 2007 Airfoil shape optimisation for transonic flows of Bethe–Zel'dovich–Thompson fluids. *AIAA J.* **45**, 1302–1316.

COURANT, R. & FRIEDRICHS, K. O. 1948 *Supersonic Flow and Shock Waves*. Interscience Publishers.

CRAMER, M. S. & FRY, R. N. 1993 Nozzle flows of dense gases. *Phys. Fluids* A **5** (5), 1246–1259.

CRAMER, M. S. & KLUWICK, A. 1984 On the propagation of waves exhibiting both positive and negative nonlinearity. *J. Fluid Mech.* **142**, 9–37.

CRAMER, M. S. & TARKENTON, G. M. 1992 Transonic flows of Bethe–Zel'dovich–Thompson fluids. *J. Fluid Mech.* **240**, 197–228.

DAFERMOS, C. M. 2005 *Hyperbolic Conservation Laws in Continuum Physics*. Springer.

DUHEM, P. 1909 On the propagation of shock waves in fluids. *Z. Phys. Chem.* **69**, 169–186.

EARNSHAW, S. 1860 On the mathematical theory of sound. *Phil. Trans. R. Soc. Lond.* **150**, 133–148.

FERGASON, S., GUARDONE, A. & ARGROW, B. 2003 Construction and validation of a dense gas shock tube. *J. Thermophys. Heat Transfer* **17** (3), 326–333.

GORI, G., VIMERCATI, D. & GUARDONE, A. 2017 Non-ideal compressible-fluid effects in oblique shock waves. *J. Phys.* **821**, 012003.

GUARDONE, A., VIGEVANO, L. & ARGROW, B. 2004 Assessment of thermodynamic models for dense gas dynamics. *Phys. Fluids* **16** (11), 3878–3887.

GUARDONE, A., ZAMFIRESCU, C. & COLONNA, P. 2010 Maximum intensity of rarefaction shock waves for dense gases. *J. Fluid Mech.* **642**, 127–146.

GUDERLEY, K. G. 1947 Considerations on the structure of mixed subsonic–supersonic flow patterns. *Air Materiel Command Technical Report* No. F-TR-2168-ND, ATI No. 22780, GS-AAF-Wright Field No. 39, U.S. Wright–Patterson Air Force Base, Dayton, OH.

GUDERLEY, K. G. 1957 *Theorie Schallnaher Strömungen*. Springer; Translated by J. R. Moszynski, Pergamon Press, 1962.

HENDERSON, L. F. & MENIKOFF, R. 1998 Triple-shock entropy theorem and its consequences. *J. Fluid Mech.* **366**, 179–210.

HUGONIOT, H. 1887 Sur la propagation du mouvement dans les corps et spécialement dans les gaz parfaits. *J. de l'Éc. Pol. Cah.* **LVII**, 97.

HUGONIOT, H. 1889 Mémoire sur la propagation du mouvement dans les corps et spécialement dans les gaz parfaits. Deuxième partie. *J. de l'Éc. Pol. Cah.* **LVIII**, 1–125.

HUNTER, J. K. & BRIO, M. 1997 Weak shock reflection. In *Proceedings of Fifth International Congress on Sound and Vibration, Adelaide, South Australia, Dec 15–18*, pp. 2023–2030. Australian Acoustical Society.

HUNTER, J. K. & BRIO, M. 2000 Weak shock reflection. *J. Fluid Mech.* **410**, 235–261.

HUNTER, J. K. & TESDALL, A. M. 2004 Weak shock reflection. In *A Celebration of Mathematical Modeling*, pp. 93–112. Springer.

JOHNSON, J. N. & CHÉRET, R. (Eds) 1998 *Classic Papers in Shock Compression Science*. Springer.

KLUWICK, A. 1991 Small-amplitude finite-rate waves in fluids having both positive and negative nonlinearity. In *Nonlinear Waves Real Fluids*, pp. 1–43. Springer.

KLUWICK, A. 1993 Transonic nozzle flow of dense gases. *J. Fluid Mech.* **247**, 661–688.

KLUWICK, A. 2001 Theory of shock waves. Rarefaction shocks. In *Handbook of Shockwaves* (ed. G. Ben-Dor, O. Igra, T. Elperin & A. Lifshitz), vol. 1, pp. 339–411. Academic.

KLUWICK, A. 2017 Non-ideal compressible fluid dynamics: a challenge for theory. *J. Phys.* **821**, 012001.

KLUWICK, A. 2018 Shock discontinuities: from classical to non-classical shocks. *Acta Mech.* **229** (2), 515–533.

KLUWICK, A. & COX, E. A. 2018 Steady small-disturbance transonic dense gas flow past two-dimensional compression/expansion ramps. *J. Fluid Mech.* **848**, 756–787.

KLUWICK, A. & KORNFELD, M. 2014 Triple-deck analysis of transonic high Reynolds number flow through slender channels. *Phil. Trans. R. Soc. Lond.* A **372** (2020), 20130346.

KLUWICK, A. & MEYER, G. 2010 Shock regularization in dense gases by viscous–inviscid interactions. *J. Fluid Mech.* **644**, 473–507.

KLUWICK, A. & MEYER, G. 2011 Viscous–inviscid interactions in transonic flows through slender nozzles. *J. Fluid Mech.* **672**, 487–520.

KREHL, P. 2001 Chapter 1-History of shock waves. In *Handbook of Shock Waves* (ed. T. E. G. Ben-Dor, O. Igra & A. Lifshitz), pp. 1–142. Academic Press.

LEE-BAPTY, I. P. & CRIGHTON, D. G. 1987 Nonlinear wave motion governed by the modified Burgers equation. *Phil. Trans. R. Soc. Lond.* A **323** (1570), 173–209.

MACH, E. 1878 Ueber den Verlauf von Funkenwellen in der Ebene und im Raume. Vienna Acad. Sitzungsberichte 78, 819.

MATHIJSSEN, T. 2017 Experimental observation of non-ideal compressible fluid dynamics: with application in organic rankine cycle power systems. PhD thesis, Delft University of Technology.

MONACO, J. F., CRAMER, M. S. & WATSON, L. T. 1997 Supersonic flows of dense gases in cascade configurations. *J. Fluid Mech.* **330**, 31–59.

NANNAN, N. R., GUARDONE, A. & COLONNA, P. 2013 On the fundamental derivative of gas dynamics in the vapor–liquid critical region of single-component typical fluids. *Fluid Phase Equilib.* **337**, 259–273.

VON NEUMANN, J. 1963*a* Oblique reflection of shocks. In *John von Neumann: Collected Works, 1903–1957, Vol 6* (ed. A. H. Taub), vol. VI, pp. 238–299. Pergamon.

VON NEUMANN, J. 1963*b* Refraction, intersection and reflection of shock waves. In *John von Neumann: Collected Works, 1903–1957, Vol. 6* (ed. A. H. Taub), vol. VI, pp. 300–308. Pergamon.

OSWATITSCH, K. 1977 *Spezialgebiete der Gasdynamik: Schallnähe, Hyperschall, Tragflächen, Wellenausbreitung*. Springer.

RANKINE, W. J. M. 1870 On the thermodynamic theory of waves of finite longitudinal disturbance. *Phil. Trans. R. Soc. Lond.* **160**, 277–288.

RUSAK, Z. & WANG, C.-W. 2000 Low-drag airfoils for transonic flow of dense gases. *Z. Angew. Math. Phys.* **51** (3), 467–480.

SCIACOVELLI, L., CINNELLA, P. & GLOERFELT, X. 2017 Direct numerical simulations of supersonic turbulent channel flows of dense gases. *J. Fluid Mech.* **821**, 153–199.

SERRE, D. 2007 Shock reflection in gas dynamics. In *Handbook of Mathematical Fluid Dynamics* (ed. S. Friedlander & D. Serre), Handbook of Mathematical Fluid Dynamics, vol. 4, chap. 2, pp. 39–122. North-Holland.

STOKES, G. G. 1848 On a difficulty in the theory of sound. *Philos. Mag.* **33**, 349–356.

TABAK, G. E. & ROSALES, R. 1994 Focusing of weak shock waves and the von Neumann paradox of oblique shock reflection. *Phys. Fluids* **6**, 1874–1892.

TESDALL, A., SANDERS, R. & POPIVANOV, N. 2015 Further results on Guderley Mach reflection and the triple point paradox. *J. Sci. Comput.* **64**, 721–744.

TESDALL, A. M. & HUNTER, J. K. 2002 Self-similar solutions for weak shock reflection. *SIAM J. Appl. Maths* **63** (1), 42–61.

THOMPSON, P. A. 1971 A fundamental derivative in gasdynamics. *Phys. Fluids* **14** (9), 1843–1849.

THOMPSON, P. A. & LAMBRAKIS, K. C. 1973 Negative shock waves. *J. Fluid Mech.* **60** (1), 187–208.

VASIL'EV, E. I. 1998 High-resolution simulation for the Mach reflection of weak shock waves. In *Proceedings of the Fourth European Computational Fluid Dynamics Conference (ECCOMAS CFD 1998, Athens, Greece)* (ed. K. D. Papailiou, D. Tsahalis, J. Periaux, Ch. Hirsch & M. Pandolfi), vol. 1, part 1, pp. 520–527. John Wiley & Sons.

VASIL'EV, E. I. & KRAJKO, A. N. 1999 Numerical simulation of weak shock diffraction over a wedge under the von Neumann paradox conditions. *Comput. Math. Math. Phys.* **39** (8), 1335–1345.

VIMERCATI, D., KLUWICK, A. & GUARDONE, A. 2018 Oblique waves in steady supersonic flows of Bethe–Zeldovich–Thompson fluids. *J. Fluid Mech.* **855**, 445–468.

WALKER, J. D. A. 1998 Turbulent boundary layers II: further developments. In *Recent Advances in Boundary Layer Theory* (ed. A. Kluwick), International Centre for Mechanical Sciences, vol. 390, pp. 145–230.

WANG, C.-W. & RUSAK, Z. 1999 Numerical studies of transonic BZT gas flows around thin airfoils. *J. Fluid Mech.* **396**, 109–141.

WRABEL, M. & KLUWICK, A. 2005 Shock boundary layer interactions in dense gases. *Proc. Annu. GAMM Meet. PAMM* **4**, 444–445.

ZELDOVICH, J. 1946 On the possibility of rarefaction shock waves. *Zh. Eksp. Teor. Fiz.* **16** (4), 363–364.